



**AUTHOR(S):**

**TITLE:**

**YEAR:**

**Publisher citation:**

**OpenAIR citation:**

**Publisher copyright statement:**

This is the \_\_\_\_\_ version of an article originally published by \_\_\_\_\_  
in \_\_\_\_\_  
(ISSN \_\_\_\_\_; eISSN \_\_\_\_\_).

**OpenAIR takedown statement:**

Section 6 of the "Repository policy for OpenAIR @ RGU" (available from <http://www.rgu.ac.uk/staff-and-current-students/library/library-policies/repository-policies>) provides guidance on the criteria under which RGU will consider withdrawing material from OpenAIR. If you believe that this item is subject to any of these criteria, or for any other reason should not be held on OpenAIR, then please contact [openair-help@rgu.ac.uk](mailto:openair-help@rgu.ac.uk) with the details of the item and the nature of your complaint.

This publication is distributed under a CC \_\_\_\_\_ license.  
\_\_\_\_\_

# 1    **Rotationally Asymmetrical Compound Parabolic** 2    **Concentrator for Concentrating Photovoltaic Applications**

3  
4    Siti Hawa Abu-Bakar<sup>a,b,\*</sup>, Firdaus Muhammad-Sukki<sup>a,c</sup>, Roberto Ramirez-Iniguez<sup>a</sup>,  
5    Tapas Kumar Mallick<sup>d</sup>, Abu Bakar Munir<sup>e,f</sup>, Siti Hajar Mohd Yasin<sup>g</sup>, Ruzairi Abdul Rahim<sup>h</sup>

6  
7    <sup>a</sup> School of Engineering & Built Environment, Glasgow Caledonian University, 70 Cowcaddens Road, Glasgow, G4 0BA Scotland, United Kingdom

8    <sup>b</sup> Universiti Kuala Lumpur British Malaysian Institute, Batu 8, Jalan Sungai Pusu, 53100 Gombak, Selangor, Malaysia

9    <sup>c</sup> Faculty of Engineering, Multimedia University, Persiaran Multimedia, 63100 Cyberjaya, Selangor, Malaysia

10    <sup>d</sup> Environment and Sustainability Institute, University of Exeter, Penryn, Cornwall, TR10 9EZ, United Kingdom

11    <sup>e</sup> Faculty of Law, University of Malaya, 50603 Kuala Lumpur, Malaysia

12    <sup>f</sup> University of Malaya Malaysian Centre of Regulatory Studies (UMCoRS), University of Malaya, 5990 Jalan Pantai Baru, Kuala Lumpur, Malaysia

13    <sup>g</sup> Faculty of Law, Universiti Teknologi MARA, 40450 Shah Alam, Malaysia

14    <sup>h</sup> Faculty of Electrical Engineering, Universiti Teknologi Malaysia, 81300 UTM Skudai, Johor, Malaysia

15  
16    \* Phone/Fax number: +44(0)141 273 1482/+44(0)141 331 3690, e-mail: [sitihawa.abubakar@gcu.ac.uk](mailto:sitihawa.abubakar@gcu.ac.uk)/[hawa012@gmail.com](mailto:hawa012@gmail.com)

17  
18        **Abstract:** This paper describes a novel type of solar concentrator – a rotationally  
19    asymmetrical compound parabolic concentrator (RACPC). The RACPC aims at addressing the  
20    following objectives: (i) to increase the electrical output of a concentrating photovoltaic (CPV)  
21    system by providing sufficient concentration gain; (ii) to minimise the usage of the PV material  
22    with the corresponding reduction of CPV system cost, and (iii) to eliminate the requirement of  
23    mechanical tracking by providing a wide field-of-view. This paper first provides a short review on  
24    variations of compound parabolic concentrator designs available to date. Next, the process of  
25    designing the RACPC is presented and the geometrical concentration gain of the concentrator is  
26    discussed. In addition, the optical concentration gain is also presented for various angles of  
27    incidence. Through simulations, it is demonstrated that the RACPC can provide significant optical  
28    concentration gains within its designed acceptance angle. An RACPC based system is an attractive  
29    alternative to conventional solar photovoltaic systems.

30  
31  
32    **Keywords:** solar photovoltaic; solar concentrator; rotationally asymmetrical compound parabolic  
33    concentrator.

36 **Nomenclatures**

37

$\theta_a$	Half-acceptance angle
$\beta_{entrance}$	Flux (in W) at the entrance aperture
$\beta_{exit}$	Flux (in W) at the exit aperture
$C_g$	Geometrical concentration gain
$C_{opt}$	Optical concentration gain
$C_{opt-eff}$	Optical efficiency
$d_0$	Exit aperture width
$d_1$	Entrance aperture width
$HTot$	Total height of the concentrator
$L_{PV}$	Length of the PV cell
$n$	Refractive index
$N$	Number of extreme rays
$W_{PV}$	Width of the PV cell
2D	Two dimensional
3D	Three dimensional
ACPC	Asymmetrical compound parabolic concentrator
BICPV	Building integrated concentrating photovoltaic
CAD	Computer-aided design
CAP	Concentration-acceptance product
CCPC	Crossed compound parabolic concentrator
CPC	Compound parabolic concentrator
CPV	Concentrating photovoltaic
DTIRC	Dielectric totally internally reflecting concentrator
EPIA	European Photovoltaic Industry Association
IGES	Initial graphics exchange specification
PV	Photovoltaic
RACPC	Rotationally asymmetrical compound parabolic concentrator

38

39

40

41

42

## 43 **1. Introduction**

44 In the last decade, solar photovoltaic (PV) has attracted significant attention worldwide due  
45 to its promising potential in addressing the world's energy needs. According to a recent report by  
46 the European Photovoltaic Industry Association (EPIA), the cumulative installed capacity of solar  
47 PV stood at 136.7 GW at the end of 2013 [1], with a world distribution as illustrated in Figure 1.  
48 More than half of the installations contributing to the cumulative total were carried out in Europe,  
49 amounting close to 80 GW. A staggering 37 GW of new solar PV capacity was installed in 2013 –  
50 an increase in 35% when compared with the installations carried out in 2012 [1]. The leading  
51 market of new solar PV installations has shifted from Europe to Asia in the last year, with China  
52 and Japan as the top 2 countries that contributed to this new installed capacity with 11 GW and 7  
53 GW respectively [1]. The rising number of solar PV installations in many countries has been mainly  
54 driven by the introduction of the feed-in tariff scheme [2]-[11]. It is reported that solar PV will  
55 continue its strong growth in 2014, with a projection of global expenditure on solar PV expected to  
56 increase by 45% in 2014 – reaching approximately \$3.8 billion [12]. The solar PV market is  
57 dominated by crystalline silicon technology at 90% of the total share, with the remaining 10%  
58 contributed by thin film technology [13].

59

60 *[Insert Figure 1 here]*

61

62 Concentrating photovoltaic (CPV) is another technology that is employed to capture solar  
63 energy. The main aim of this technology is to reduce the cost of solar PV systems by minimising  
64 the usage of expensive PV material in the system design. This is achieved by incorporating an  
65 optical device that concentrates the sunlight onto a smaller area where a PV cell is attached [14]. By  
66 2014 CPV contributes only with 357.9 MW to the total installed capacity - led by China and  
67 America [15]. However, according to GlobalData, the CPV market will 'expand dramatically' in the  
68 next few years, and is projected to reach 1GW in 2020 [15]. These installations are normally carried  
69 out in large solar power plant, but recently there has been a significant rise in the use of CPV for  
70 building integration applications including sky lights, double glazing windows and solar blinds  
71 [16]-[18]. This concept is widely known as building integrated concentrating photovoltaic  
72 (BICPV).

73

74 Researchers have produced various types of concentrators for CPV purposes [16],[19]-[30] .  
75 One of the most popular is known as the compound parabolic concentrator (CPC) and has been  
76 explored for various applications since 1960s [31]. The basic geometry of a CPC is shown in Figure  
2. It can be divided into three parts; a planar entrance aperture ( $AB$ ), two totally internally reflecting

77 or reflective side profiles which consist of segments of parabolas ( $AC$  and  $BD$ ) and an exit aperture  
78 ( $CD$ ). The CPC has a half-acceptance angle<sup>1</sup> of  $\theta_a$  and concentrates all the incoming sun rays  
79 within its half-acceptance angle to the exit aperture  $CD$  [31].

80

81 *[Insert Figure 2 here]*

82

83 To date, there is a variety of CPCs that have been studied (see Table 1). The two most  
84 common designs of CPC are the 2D linear [33] and the 3D rotational symmetry [34]. The 2D  
85 design is produced by extruding the cross section of a symmetrical CPC along the axis  
86 perpendicular to the 2D cross section - creating a square or rectangular exit aperture. As for the 3D  
87 rotational symmetry design, the 2D cross section design is rotated around the optical axis of the  
88 CPC which will have circular entrance and exit apertures. These concentrators can be fabricated  
89 from reflective materials such as mirrors or from solid dielectric materials. According to Welford  
90 and Winston [31], a concentrator fabricated using a solid dielectric material offers additional  
91 practical advantages such as ensuring 100% efficient total internal reflection on the side wall,  
92 producing a wider half-acceptance angle as well as creating a more compact concentrator.

93 Benitez et al. [35] indicates that the performance of any concentrator can be evaluated by  
94 using the concentration-acceptance product (CAP) formulae, which are defined as follow:

95

96 For the 2D design [35], the CAP is defined as

$$CAP_{2D} = C_{g(2D)} \sin(\theta_a) \quad (2)$$

97

98 while for the 3D design [35], it is defined as

$$CAP_{3D} = \sqrt{C_{g(3D)}} \sin(\theta_a) \quad (3)$$

99

100 where  $C_g$  is the geometrical concentration gain<sup>2</sup> and  $\theta_a$  is the half-acceptance angle of the  
101 concentrator. The CAP value is governed by thermodynamic upper bound limit of equal to the value

---

<sup>1</sup> The half-acceptance angle is defined as the angle where at least 90% of the rays entering the entrance aperture emerge from the exit aperture of the concentrator [16],[31].

<sup>2</sup> Geometrical concentration gain of a 2D concentrator is defined as the ratio of the width of the entrance aperture to the width of the exit aperture [31]. As for a 3D concentrator, this parameter is defined as the area ratio of the entrance aperture to the exit aperture [31].

102 of the refractive index of the material,  $n$ . In theory, a concentrator with a higher CAP value  
103 performs better than a concentrator having a lower CAP value. It is therefore desirable to have a  
104 design that has a CAP value closer to the value of index of refraction.

105  
106 *[Insert Table 1 here]*  
107

108 Ronnelid et al. [36] investigated the performance of a 2D extrusion of a symmetrical CPC  
109 fabricated from a reflective aluminium foil. The CPC has a geometrical concentration gain of 1.53,  
110 an exit aperture width of 14.4 cm, a total height of 12 cm and a half-acceptance angle of 35°. From  
111 the simulations, it was found that the CPC-collector could increase the annual energy output by  
112 2.6% when compared with the non-concentrating system. This concentrator has a CAP of 0.88. Pei  
113 et al. [37] on the other hand, studied the performance of a 2D extrusion of a symmetrical dielectric  
114 CPC. The CPC has a geometrical concentration gain of 2.41, an exit aperture width of 1 cm, total  
115 height of 2.7 cm and a half-acceptance angle of 36.8°. It is calculated that the CAP of the  
116 concentrator is 1.44. Based on their experiments, they concluded that the introduction of a dielectric  
117 CPC increased the electrical power from 25.86 mW to 44.80 mW when compared with non-  
118 concentrating PV, an increment of about 73%.

119 Cooper et al. [38] utilised a reflective 3D rotationally symmetric CPC that has a half-  
120 acceptance angle of 30°. From their ray tracing analysis, they found that the transmission-angle  
121 curve of the reflective design produced an almost ideal step-like behavior within its designed  
122 acceptance angle. Goodman et al. [39] analysed the performance of a 3D rotationally symmetric  
123 dielectric CPC with a geometrical concentration gain of 6.1, a half-acceptance angle of 10°. The  
124 CAP is calculated to be 0.43. From the experiment, the cell coupled with this CPC design produced  
125 a 5.7 more short circuit current when compared with a bare solar cell.

126 Mallick et al. [40] also demonstrated another variation of a CPC design known as the  
127 asymmetrical compound parabolic concentrator (ACPC). Unlike the symmetrical 2D CPC, the two  
128 segments of the ACPC consist of two different lengths of parabola which allows the final design to  
129 have a wider acceptance angle. The concentrator has a geometrical concentration gain of 2 and is  
130 fabricated from a reflective material. Based on the experiments, their results point out that this  
131 concentrator managed to increase the maximum electrical output power by 62% when compared  
132 with a non-concentrating system – achieving a maximum optical efficiency<sup>3</sup> of 85.85%. Sarmah et

---

<sup>3</sup> An optical efficiency measures the fraction of the rays that is transmitted from the entrance aperture of the concentrator to the exit aperture of the concentrator [31].

133 al. [41] researched on a dielectric ACPC having a geometrical concentration gain of 2.8. Their  
134 analysis showed that the design has a maximum optical efficiency of 80.5% and increased the  
135 electrical power ratio to 2.27 when compared with a system without a concentrator.

136 Mammo et al. [42] constructed a reflective 3D crossed compound parabolic concentrator  
137 (CCPC)-based photovoltaic module. A CCPC is formed by intersecting two extrusions of linear  
138 symmetrical CPC orthogonally. With a geometrical concentration gain of 3.61, a half-acceptance  
139 angle of  $30^\circ$ , a total height of 1.616 cm and a square 1 cm by 1 cm exit aperture, this design is  
140 capable of generating a maximum electrical power concentration of 3 when compared to similar  
141 type of non-concentrating module. This concentrator has a CAP of 0.95. Baig et al. [43] fabricated  
142 the previous concentrator design by using a dielectric material known as polyurethane having a  
143 refractive index of 1.5, and evaluated its performance. The dielectric CCPC design has a maximum  
144 optical efficiency of 73.4%, a half-acceptance angle of  $35^\circ$  and produced a maximum electrical  
145 power ratio of 2.67 when compared with the non-concentrating design. As for the CAP, the value is  
146 calculated to be 1.09.

147 This paper proposes a new type of CPC design for use in BIPV systems. This concentrator  
148 is known as a rotationally asymmetrical compound parabolic concentrator (RACPC). Section 2  
149 explains the steps involved in producing this design, and the geometrical properties of the RACPC  
150 are presented in Section 3. The optical concentration gain analysis is carried out in Section 4 to  
151 evaluate the angular performance of the concentrator. Afterwards, the annual output prediction of  
152 an RACPC based panel is presented in Section 5. Conclusions are presented at the end of the paper.

## 153 154 **2. Design of the RACPC**

155  
156 The RACPC is a new variation of the CPC and can be constructed from dielectric material.  
157 The foundation and the algorithms to produce this concentrator are based on the concentrator  
158 design proposed by Ning et al. [28] for the dielectric totally internally reflecting concentrator  
159 (DTIRC). According to Ning et al. [28], the CPC is a specific case of the DTIRC family with a flat  
160 entrance aperture.

161 A MATLAB® based program has been developed to create the RACPC. The flow chart of  
162 the program is summarised in Figure 3 while the illustration of the creation process is presented in  
163 Figure 4. The RACPC design requires of the following input parameters: the total height of the  
164 concentrator, ( $HT_{tot}$ ), the half-acceptance angle ( $\theta_a$ ), the length of the PV cell ( $L_{PV}$ ), the width of the  
165 PV cell ( $W_{PV}$ ), the trial width of the entrance aperture ( $d_I$ ), the index of refraction of the material ( $n$ )  
166 and the number of extreme rays ( $N$ ).

167 *[Insert Figure 3 here]*

168

169 *[Insert Figure 4 here]*

170

171 First, based on the input parameters, a 2D symmetrical design is produced (see position ‘1’ in  
172 Figure 4). The computer program calculates the trial height, which is later used to calculate the  
173 coordinates of the side wall of the parabola. This calculation takes into account a number of  
174 extreme rays entering the concentrator at the critical angle. Once it is completed, the program  
175 compares the trial entrance aperture to the calculated entrance aperture. The difference between the  
176 two apertures is used to adjust the trial entrance aperture. A number of iterations take place until the  
177 difference between both entrance apertures is within an acceptable error value. The calculated total  
178 height of the concentrator is then compared with the desired total height and is adjusted by varying  
179 the half-acceptance angle until the difference between the two total heights is within an acceptable  
180 error value. These steps will define the 2D design in position '1'. The process is repeated to get the  
181 next 2D cross-section design (see position ‘2’ in Figure 4). Each new design is computed by  
182 incrementing the angle of rotation of the cross-sections by 1° and using the predetermined exit  
183 aperture value. The process stops when a 180° rotation around the y-axis is completed. The  
184 program calculates three output parameters; the ‘final’ half-acceptance angle, the ‘final’ width of  
185 entrance aperture and the geometrical concentration gain of the concentrator. The program also  
186 saves all the coordinates of the design in a point cloud format for fabrication purposes.

187

188 The RACPC shown in Figure 5 is generated by selecting the total height  $HTot$  of 3.0 cm, a  
189 refractive index  $n$  of 1.5 and the exit aperture with dimensions of 1 cm by 1 cm. The geometry of  
190 the concentrator has distinctive features when compared with other CPCs. First, the planar entrance  
191 aperture has four axis of symmetry (see Figure 5(b)), unlike the 3D rotationally symmetry CPC or  
192 the CCPC which has a circular and square shape respectively. Another important feature of this  
193 concentrator is its square exit aperture, as presented in Figure 5(c). Sellami et al. [16] argued that  
194 the circular entrance and exit apertures of a traditional rotationally symmetry CPC exhibit losses  
195 which reduce the optical efficiency of the concentrator. They also indicate that from a  
196 manufacturing point of view, it is more desirable and easier to fabricate a square or a rectangular  
197 cell, which is widely available shape in the market, than a circular cell required in a rotationally  
198 symmetry design. The RACPC is also a variation of a 3D design, therefore it provides a higher  
199 geometrical concentration gain than the 2D linear CPC design of a symmetrical CPC.

199

200 *[Insert Figure 5 here]*



### 3. Geometrical Concentration Gain Analysis

This section investigates the effect of varying the total height and the refractive index of the concentrator on both the geometrical concentration gain and the half-acceptance angle of the RACPC. The geometrical concentration gain,  $C_g$  of a 3D concentrator is defined as the area ratio of the entrance aperture to the exit aperture of the concentrator [31]. It has been indicated in Section 2 that the MATLAB® program requires certain input parameters and returns three main output parameters which are the geometrical gain, the ‘final’ half-acceptance angle and the ‘final’ length of the entrance aperture. This information is valuable in estimating the final optoelectronic gain based on the input parameters as well as constructing and assembling the optimum RACPC design for BICPV applications.

Figure 6 shows some of the properties of RACPCs generated with various total heights and different refractive indices, where the variation of geometrical concentration gain and the half-acceptance angle are presented in Figures 6(a) and 6(b) respectively. From Figure 6(a), it can be observed that the geometrical concentration gain varies between 1.7299 and 6.5920. In general, the geometrical concentration gain increases as the total height of the concentrator increases. In Figure 6(b), the half-acceptance angle of the RACPC varies from 25.9183° to 55.3914°. From these observations, it can be concluded that when the height of the concentrator (and the gain) increases, the half-acceptance angle reduces. In terms of index of refraction, it can also be seen that both the geometrical concentration gain and the half-acceptance angle vary increase when the index of refraction of the material increases, as illustrated in Figure 6. For two concentrators with the same height, the one fabricated with a higher index of refraction has a higher geometrical concentration gain and larger half-acceptance angle. These three behaviours support the findings by Ning et al. [28] and Muhammad-Sukki et al. [19],[22]-[25].

*[Insert Figure 6 here]*

### 4. Optical Concentration Gain Analysis

Another important aspect to investigate is the optical concentration gain. The optical concentration gain,  $C_{opt}$  is defined as [16],[31]:

$$C_{opt} = \frac{\beta_{exit}}{\beta_{entrance}} \times C_g \quad (1)$$

233

234 where  $\beta_{exit}$ ,  $\beta_{entrance}$  and  $C_g$  are the flux (in W) at the exit aperture, the flux (in W) at the entrance  
235 aperture and the geometrical concentration gain respectively. The ratio of the flux at the entrance  
236 aperture to the flux at the exit aperture is also known as the optical efficiency,  $C_{opt-eff}$  of a  
237 concentrator [34],[41]. In theory, any rays within the acceptance angle of the concentrator will  
238 emerge at the exit aperture of the concentrator [31]. The analysis evaluates the gain performance of  
239 the concentrator when exposed to rays at different angles of incidence. This is useful to predict the  
240 theoretical performance of the RACPC when exposed to the sun.

241 First, the 3-D surface coordinates of an RACPC are generated from MATLAB® in a point  
242 cloud format. This file is then imported into GeoMagic® software to produce a computer-aided  
243 design (CAD) model from which an Initial Graphics Exchange Specification (IGES) format file  
244 model is obtained, such as the one illustrated in Figure 5. Subsequently, this IGES file is imported  
245 into an optical system design software called ZEMAX® to conduct the ray tracing analysis. A  
246 simulation using any optical system design software such as ZEMAX® is better than using a  
247 programming software (i.e. MATLAB®) because [44]: (i) it gives flexibility in analysing any  
248 optical devices; (ii) it can analyse a greater number of incoming rays which results in better  
249 resolution of the optical flux distribution; (iii) it shortens the simulation times significantly, and (iv)  
250 it provides better result representations at the end of the simulation.

251 The setup for the ray tracing analysis in ZEMAX® is shown in Figure 7. A square light  
252 source is selected to produce one million collimated rays and is configured to produce an incoming  
253 power of 1,000 W. The IGES file of the RACPC is placed at a distance of 35 cm from the light  
254 source. To calculate the number of rays at the entrance and exit aperture of the RACPC, two photo  
255 detectors are attached at both ends of the concentrator. The simulation is carried out by first, firing  
256 the rays perpendicular to the concentrator where the number of rays at the entrance and exit  
257 apertures are calculated and recorded. This is repeated by increasing the rays' incidence angle by 5°  
258 until a maximum angle of 60° is reached.

259

*[Insert Figure 7 here]*

260

261 Figure 8 shows the optical concentration gain variation of several RACPC designs when the  
262 total height is varied from 2 cm to 5 cm and the refractive index is varied from 1.30 to 1.50. From  
263 the simulations, it is observed that the concentrator provides a substantial gain within its half-  
264 acceptance angle (in this example it can reach up to 6.18), and the optical concentration gain  
265 reduces when the angle of incidence is beyond the half-acceptance angle. A comparison between  
266 the half-acceptance angle values generated from the ZEMAX® simulation and the one generated

267 from the MATLAB® simulations is presented in Table 2. Interestingly, the value of the half-  
268 acceptance angle obtained from the ZEMAX® simulations agrees with calculated half-acceptance  
269 angle from the MATLAB® simulation with a small percentage variation of between -0.32% and  
270 7.62%. The CAP value is also calculated and included in Table 2. The CAP value is always less  
271 than the index of refraction and ranges between 0.88 and 1.32.

272

273 *[Insert Figure 8 here]*

274

275 *[Insert Table 2 here]*

276

277 It can be concluded that the trend of optical concentration gain is similar to the geometrical  
278 concentration gain analysis, where the optical concentration gain increases when the total height of  
279 the concentrator increases. This is also true in terms of the refractive index of the concentrator  
280 material, where the optical concentration gain is higher when the refractive index of the  
281 concentrator is higher for the same total height.

282 It is therefore pertinent to know that some trade off needs to be made when choosing the  
283 optimum RACPC design for the BICPV system. A higher gain is often desirable but this translates  
284 into a taller concentrator and smaller acceptance angle - this means that the RACPC design will  
285 only gather sun light for a shorter period of time during the day.

286 It is also important to investigate the variation of irradiance distribution on the solar cell  
287 when incorporating different RACPC designs. It has been reported by various researchers that an  
288 increase in concentration for a long period of time increases the temperature of the solar cell, and  
289 eventually reduces the electrical output of the system [25],[42]-[44]. Figure 9 shows the distribution of  
290 irradiance on the solar cell when three different RACPC designs having the same refractive index of  
291 1.40 are simulated at normal angle of incidence. Based on the conditions indicated earlier in Section 4,  
292 a typical solar cell has a maximum peak irradiance of  $16.7 \text{ W/cm}^2$ , as illustrated in Figure 9(a). As for  
293 the RACPC, the irradiance distribution is concentrated at the four corners of the solar cell. The  
294 maximum peak irradiance reaches up to  $70 \text{ W/cm}^2$ ,  $90 \text{ W/cm}^2$  and  $140 \text{ W/cm}^2$  when the total height of  
295 the RACPC increases to 3 cm, 4 cm and 5 cm respectively. This translates into an increment of 4x, 5x  
296 and 8x respectively when compared with the peak irradiance on a non-concentrating cell. It is  
297 therefore crucial for a BICPV system to have the right RACPC design and cooling system to ensure  
298 that the performance of the solar cell is at its optimum. If an RACPC design with higher gain is  
299 needed, the solar cell could be cooled by introducing a hybrid/thermal system (either using air or  
300 water), that utilises the co-generated heat to produce hot water and stimulate ventilation [19],[25],[45].

301 *[Insert Figure 9 here]*

302  
303 **5. Annual output prediction**

304  
305 It is desirable to predict the annual electrical output (in kWh) generated from the CPV  
306 system utilising the RACPC design and compare it with a conventional non-concentrating PV  
307 skylight. The comparison is carried out based on the area (in square meter) of solar cell used to  
308 produce a 1m<sup>2</sup> PV skylight. One particular design of RACPC is chosen, with a total height of 3 cm  
309 and fabricated from a material with a refractive index of 1.5. Figure 10 shows an example of the  
310 CPV design that incorporates the chosen RACPC concentrator. To simplify the analysis, the  
311 following assumptions are made: (i) the solar cell conversion efficiency is 17.32%<sup>4</sup>; (ii) the panels  
312 are installed near the Malaysian Meteorological Department in Kuala Terengganu, Malaysia  
313 (5°22'48"N, 103°00'00"E); (iii) the panels are mounted on a south facing rooftop at an angle of 5°  
314 from the horizontal to match the latitude of the site [46], and (iv) the panels are static, i.e. no  
315 mechanical tracking system is attached on any panel. Based on the average daily solar irradiance  
316 data in Kuala Terengganu, Malaysia [47], the variation of sun path throughout the year [46] and the  
317 daily optical concentration gain from the ZEMAX® simulation, the energy yield from both panels  
318 are calculated.

319  
320 *[Insert Figure 10 here]*

321  
322 Figure 11 shows the annual energy output from the RACPC panel and the conventional PV  
323 skylight. The RACPC panel produces 220 kWh per year, in contrast to the traditional PV skylight  
324 which only generates about 67.75 kWh per year. It can be seen that the RACPC based panel could  
325 increase the electrical output by 3.25 times (225%) when compared with amount generated by the  
326 non-concentrating counterpart. It is important to mention here that these calculations only predict  
327 the annual electricity output generated by the two panels.

328 Another advantage of the concentrator is that it could provide natural ambient light for  
329 building interiors due to the fact that the material used for the concentrator is transparent, which  
330 could potentially reduce the energy consumption and electricity cost for lighting purposes. Also, the  
331 cogenerated heat from the cooling system of the cell could be used for heating and/or to stimulate

---

<sup>4</sup> This is based on the efficiency of the cell used during the experiments carried out by Muhammad-Sukki et al. [24].

332 ventilation, which also reduces the electricity requirements in a building.

333

334

[Insert Figure 11 here]

335

336

### 337 **Conclusions**

338

339 A new type of concentrator, known as the RACPC has been created for use in BICPV  
340 systems. The steps to produce the RACPC have been discussed and both the geometrical  
341 concentration gain and the optical concentration gain are evaluated. From the simulations, it has  
342 been found that the RACPC could produce an optical concentration gain as high as 6.18 when  
343 compared with the non-concentrating cell depending on the half-acceptance angle. It can be  
344 concluded that a BICPV system incorporating this RACPC would not only generate electricity  
345 efficiently, but also minimise energy consumption in buildings by providing ambient light to  
346 building interiors, and using the cogenerated heat for heating and stimulating ventilation which  
347 could provide greener and sustainable building. The authors are currently fabricating a specific  
348 RACPC design to evaluate its actual performance.

349

350

### 351 **Acknowledgments**

352

353 This project is funded by Glasgow Caledonian University (GCU), Scotland's Energy  
354 Technology Partnership (ETP) and Majlis Amanah Rakyat (MARA), Malaysia. The authors would  
355 like to acknowledge the collaboration of AES Ltd. for its contribution to this project.

356

357

### 358 **References**

359

[1]. European Photovoltaic Industry Association (EPIA), 2014. Market report 2013. EPIA, Belgium.

360

[2]. Muhammad-Sukki F, Abu-Bakar SH, Munir AB, Mohd Yasin SH, Ramirez-Iniguez R, McMeekin SG,  
361 Stewart BG, Sarmah N, Mallick TK, Abdul Rahim R, Karim ME, Ahmad S. & Mat Tahar R. Feed-in tariff for  
362 solar photovoltaic: The rise of Japan. *Renewable Energy* 2014; **68**: 636-643.

363

[3]. Muhammad-Sukki F, Abu-Bakar SH, Munir AB, Mohd Yasin SH, Ramirez-Iniguez R, McMeekin SG,  
364 Stewart BG & Abdul Rahim R. Progress of feed-in tariff in Malaysia: A year after. *Energy Policy* 2014; **67**:

365

618-625.

- 366 [4]. Muhammad-Sukki F, Abu-Bakar SH, Munir AB, Mohd Yasin SH, Ramirez-Iniguez R, McMeekin SG,  
 367 Stewart BG & Abdul Rahim R. Feed-in tariff in Malaysia: Six month after. *Proceedings of Sustainable Future*  
 368 *Energy 2012 & 10th Sustainable and Secure Energy (SEE) Forum 2012*: 452-458.
- 369 [5]. Muhammad-Sukki F, Munir AB, Ramirez-Iniguez R, Abu-Bakar SH, Mohd Yasin SH, McMeekin SG &  
 370 Stewart BG. Solar photovoltaic in Malaysia: The way forward. *Renewable and Sustainable Energy Reviews*  
 371 2012; **16(7)**: 5232-5244.
- 372 [6]. Muhammad-Sukki F, Munir AB, Ramirez-Iniguez R, Abu-Bakar SH, Mohd Yasin SH, McMeekin SG,  
 373 Stewart BG & Anuar K. Soft loan for domestic installation of solar photovoltaic in Malaysia: Is it the best  
 374 option?. *Proceedings of IEEE Business Engineering and Industrial Applications Colloquium 2012*: 388-393.
- 375 [7]. Munir AB, Mohd Yasin SH, Muhammad-Sukki F, Abu-Bakar SH & Ramirez-Iniguez R. Feed-in tariff for  
 376 solar photovoltaic: Money from the sun?. *Malayan Law Journal*; **2**: lvii-lxxii.
- 377 [8]. Mohd Yasin SH, Munir AB, Muhammad-Sukki F, Abu-Bakar SH & Ramirez-Iniguez R. Feed-in tariff:  
 378 Money from the sun?. *Proceedings of International Conference on Emerging Issues in Public Law:*  
 379 *Challenges and Perspectives 2011*: 1- 13.
- 380 [9]. Muhammad-Sukki F, Ramirez-Iniguez R, Abu-Bakar SH, McMeekin SG & Stewart BG. An evaluation of the  
 381 installation of solar photovoltaic in residential houses in Malaysia: Past, present and future. *Energy Policy*  
 382 2011; **39(12)**: 7975–7987.
- 383 [10]. Muhammad-Sukki F, Ramirez-Iniguez R, Abu-Bakar SH, McMeekin SG, Stewart BG & Chilukuri MV.  
 384 *Proceedings of 5th International Power Engineering and Optimization Conference 2011*: 221-226.
- 385 [11]. Muhammad-Sukki F, Ramirez-Iniguez R, Munir AB, Mohd Yasin SH, Abu-Bakar SH, McMeekin SG &  
 386 Stewart BG. Revised feed in tariff for solar photovoltaic in the United Kingdom: A cloudy future ahead?.  
 387 *Energy Policy* 2012; **52(1)**: 832-838.
- 388 [12]. PV Magazine, 2014. Solar spending could reach \$3.8bn in 2014, says IHS. PV Magazine. Last accessed on  
 389 22/05/2014. Available from [http://www.pv-magazine.com/news/details/beitrag/solar-spending-could-reach-38bn-in-2014--says-ihs\\_100014581/#ixzz32RHiRwd5](http://www.pv-magazine.com/news/details/beitrag/solar-spending-could-reach-38bn-in-2014--says-ihs_100014581/#ixzz32RHiRwd5)
- 390 [13]. Four Peaks Technologies, 2014. Solar markets. Four Peaks Technologies, USA. Last accessed on 22/05/2014.  
 391 Available from [http://solarcellcentral.com/markets\\_page.html](http://solarcellcentral.com/markets_page.html)
- 392 [14]. Muhammad-Sukki F, Ramirez-Iniguez R, McMeekin SG, Stewart BG & Clive B. Solar concentrators.  
 393 *International Journal of Applied Sciences* 2010; **1(1)**: 1-15.
- 394 [15]. PV Magazine, 2014. Global CPV capacity expected to reach 1 GW by 2020. PV Magazine. Last accessed on  
 395 22/05/2014. Available from [http://www.pv-magazine.com/news/details/beitrag/global-cpv-capacity-expected-to-reach-1-gw-by-2020\\_100014547/#ixzz32RQEZKIH](http://www.pv-magazine.com/news/details/beitrag/global-cpv-capacity-expected-to-reach-1-gw-by-2020_100014547/#ixzz32RQEZKIH)
- 396 [16]. Sellami N, Mallick TK & McNeil DA. Optical characterization of 3-D static solar concentrator. *Energy*  
 397 *Conversion and Management* 2012; **64**: 579-586.
- 398 [17]. Baig H & Mallick TK, Challenges and opportunities in concentrating photovoltaic research. *Modern Energy*  
 399 *Review* 2011; **3(2)**: 20-26.
- 400 [18]. Norton B, Eames PC, Mallick TK, Huang MJ, McCormack SJ & Mondol JD. Enhancing the performances of  
 401 building integrated photovoltaics. *Solar Energy* 2011; **85(8)**: 1629-1664.
- 402 [19]. Muhammad-Sukki F, Ramirez-Iniguez R, McMeekin SG, Stewart BG & Clive B. Optimised dielectric totally  
 403 internally reflecting concentrator for the solar photonic optoelectronic transformer system: Maximum  
 404  
 405



- 406 concentration method. In: Setchi R, Jordanov I, Howlett RJ & Jain LC, editors. *Knowledge-Based and*  
407 *Intelligent Information and Engineering Systems 2010*; 6279(4): 633-641.
- 408 [20]. Muhammad-Sukki F, Ramirez-Iniguez R, McMeekin SG, Stewart BG & Clive B. Solar concentrators in  
409 Malaysia: Towards the development of low cost solar photovoltaic systems. *Jurnal Teknologi* 2011; **55(1)**: 53-  
410 65.
- 411 [21]. Muhammad-Sukki F, Ramirez-Iniguez R, McMeekin SG, Stewart BG & Clive B. Optimised concentrator for  
412 the Solar Photonic Optoelectronic Transformer: Optical concentration gain analysis. Proceedings of *IET*  
413 *Renewable Power Generation Conference 2011*; P4: 1-6.
- 414 [22]. Muhammad-Sukki F, Ramirez-Iniguez R, McMeekin SG, Stewart BG & Clive B. Optimisation of concentrator  
415 in the Solar Photonic Optoelectronic Transformer: Comparison of geometrical performance and cost of  
416 implementation. *Renewable Energy and Power Quality Journal* 2011; Reference Paper No. 436: 1-6.
- 417 [23]. Muhammad-Sukki F, Ramirez-Iniguez R, McMeekin SG, Stewart BG & Clive B. Optimised concentrator for  
418 the Solar Photonic Optoelectronic Transformer System: First optimisation stage. *Caledonian Journal of*  
419 *Engineering* 2011; **7(1)**: 19-24.
- 420 [24]. Muhammad-Sukki F, Abu-Bakar SH, Ramirez-Iniguez R, McMeekin SG, Stewart BG, Munir AB, Mohd  
421 Yasin SH, & Abdul Rahim R. Performance analysis of a mirror symmetrical dielectric totally internally  
422 reflecting concentrator for building integrated photovoltaic systems. *Applied Energy* 2013; **111**: 288-299.
- 423 [25]. Muhammad-Sukki F, Abu-Bakar SH, Ramirez-Iniguez R, McMeekin SG, Stewart BG, Sarmah N, Mallick  
424 TK, Munir AB, Mohd Yasin SH, & Abdul Rahim R. Mirror symmetrical dielectric totally internally reflecting  
425 concentrator for building integrated photovoltaic systems. *Applied Energy* 2014; **113**: 32-40.
- 426 [26]. Ramirez-Iniguez R, Muhammad-Sukki F, Abu-Bakar SH, McMeekin SG, Stewart BG, Sarmah N, Mallick  
427 TK, Munir AB, Mohd Yasin SH, & Abdul Rahim R. Rotationally asymmetric optical concentrators for solar  
428 PV and BIPV systems. Proceedings of *4<sup>th</sup> International Conference on Photonics 2013*; 15-17.
- 429 [27]. Ramirez-Iniguez R, Muhammad-Sukki F, McMeekin SG & Stewart BG. Optical element. UK Patent  
430 Application No. GB1122136.3, 2013.
- 431 [28]. Ning X, Winston R & O’Gallagher J. Dielectric Totally Internally Reflecting Concentrators. *Applied Optics*  
432 1987; **26(2)**: 300–305.
- 433 [29]. Chemisana D, Collados MV, Quintanilla M & Atencia J. Holographic lenses for building integrated  
434 concentrating photovoltaics. *Applied Energy* 2013; **110**: 227-235.
- 435 [30]. Uemetsu T, Warabikaso T, Yazawa Y & Muramatsu S. Static micro-concentrator photovoltaic module with an  
436 acorn shape reflector. Proceedings of *World Conference on Photovoltaic Solar Energy Conversion 1998*;  
437 1570-1573.
- 438 [31]. Welford WT & Winston R. *High Collection Nonimaging Optics*. 1st edn. USA. Academic Press Inc. 2000.
- 439 [32]. Gudekar AS, Jadhav AS, Panse SV, Joshi JB & Pandit AB. Cost effective design of compound parabolic  
440 collector for steam generation. *Solar Energy* 2013; **90**: 43-50.
- 441 [33]. Winston R. Principles of solar concentrator of a novel design. *Solar Energy* 1974; **16**: 89-95.
- 442 [34]. Winston R. Dielectric compound parabolic concentrators. *Applied Optics* 1976; **15(2)**: 291-292.
- 443 [35]. Benítez P, Miñano JC, Zamora P, Mohedano R, Cvetkovic A, Buljan M, Chaves J & Hernández M. High  
444 performance Fresnel-based photovoltaic concentrator. *Optics Express* 2010; **18(S1)**: A25–A40.

- 445 [36]. Rönnelid M, Perers B & Karlsson B. Construction and testing of a large-area CPC-collector and comparison  
446 with a flat plate collector. *Solar Energy* 1996; **57(3)**: 177-184.
- 447 [37]. Pei G, Li G, Su Y, Ji J, Riffat S, Zheng H. Preliminary ray tracing and experimental study on the effect of  
448 mirror coating on the optical efficiency of a solid dielectric compound parabolic concentrator. *Energies* 2012;  
449 **5(9)**:3627-3639.
- 450 [38]. Cooper T, Dähler F, Ambrosetti G, Pedretti A & Steinfeld A. Performance of compound parabolic  
451 concentrators with polygonal apertures. *Solar Energy* 2013; **95**: 308-318.
- 452 [39]. Goodman NB, Ignatius R, Wharton L & Winston R. Solid-dielectric compound parabolic concentrators: On  
453 their use with photovoltaic devices. *Applied Optics* 1976; **15**: 2434-2436.
- 454 [40]. Mallick TK, Eames PC & Norton B. Non-concentrating and asymmetric compound parabolic concentrating  
455 building façade integrated photovoltaics: An experimental comparison. *Solar Energy* 2006; **80(7)**: 834-849.
- 456 [41]. Sarmah N, Richards BS & Mallick TK. Design, development and indoor performance analysis of a low  
457 concentrating dielectric photovoltaic module. *Solar Energy* 2014; **103**: 390-401.
- 458 [42]. Mammo ED, Sellami N & Mallick TK. Performance analysis of a reflective 3D crossed compound parabolic  
459 concentrating photovoltaic system for building façade integration. *Progress in Photovoltaic: Research and  
460 Applications* 2013; **21**:1095-1103.
- 461 [43]. Baig H, Sellami N, Chemisana D, Rosell J & Mallick TK. Performance analysis of a dielectric based 3D  
462 building integrated concentrating photovoltaic system. *Solar Energy* 2014; **103**: 525-540.
- 463 [44]. Sellami N. Design and characterisation of a novel translucent solar concentrator. PhD Thesis, Heriot-Watt  
464 University 2013.
- 465 [45]. Kumar R & Rosen MA. A critical review of photovoltaic-thermal solar collectors for air heating. *Applied  
466 Energy* 2011; **88**: 3603-3614.
- 467 [46]. Boxwell M. *Solar electricity handbook*. 1<sup>st</sup> edn. USA. Green Stream Publishing. 2010.
- 468 [47]. Muzathik AM, Wan Nik WMN, Samo K, & Ibrahim MZ. Hourly global solar radiation estimates on a  
469 horizontal plane. *Journal of Physical Science* 2010; **21(2)**: 51–66.
- 470
- 471



## Figures and Tables descriptions

Figure	Description	Proposed size (width)
1	Cumulative solar PV installed capacity in 2013. Adapted from [1].	90mm
2	A cross section of a CPC. Adapted from [32].	90mm
3	The flowchart of producing an RACPC.	140mm
4	Demonstration of the angular rotation of the 2-D cross-sections to produce the RACPC.	90mm
5	An example of an RACPC ( $HT_{tot} = 3.0$ cm and $n = 1.30$ ), where (a) is the isometric view; (b) is the top view; (c) is the bottom view, and (d) the side view of the concentrator.	140mm
6	Geometrical properties of the RACPC generated from various total heights and different refractive indices where (a) the geometrical concentration gain, and (b) the half-acceptance angle of the concentrator.	90mm
7	Ray tracing analysis conducted in ZEMAX®.	90mm
8	Optical concentration gain of various RACPC presented with various total heights and refractive indices.	140mm
9	Photodetector's results obtained from the ZEMAX® simulation of concentration distribution at the detector of (a) non-concentrating cell; (b) RACPC with $HT_{tot} = 3$ cm; (c) RACPC with $HT_{tot} = 4$ cm, and (d) RACPC with $HT_{tot} = 5$ cm. All the concentrators are fabricated using $n = 1.40$ . The unit is recorded in $W/cm^2$ .	140mm
10	Aerial view of the arrangement of RACPCs in a module (not to scale).	90mm
11	Annual performance of the RACPC and the traditional PV skylight.	90mm

Table	Description	Proposed size (width)
1	Summary of various CPC designs that have been studied.	190mm
2	Comparison of acceptance angle values generated from the ZEMAX® simulation and from MATLAB® simulation.	190mm

Figure 1  
Click here to download high resolution image

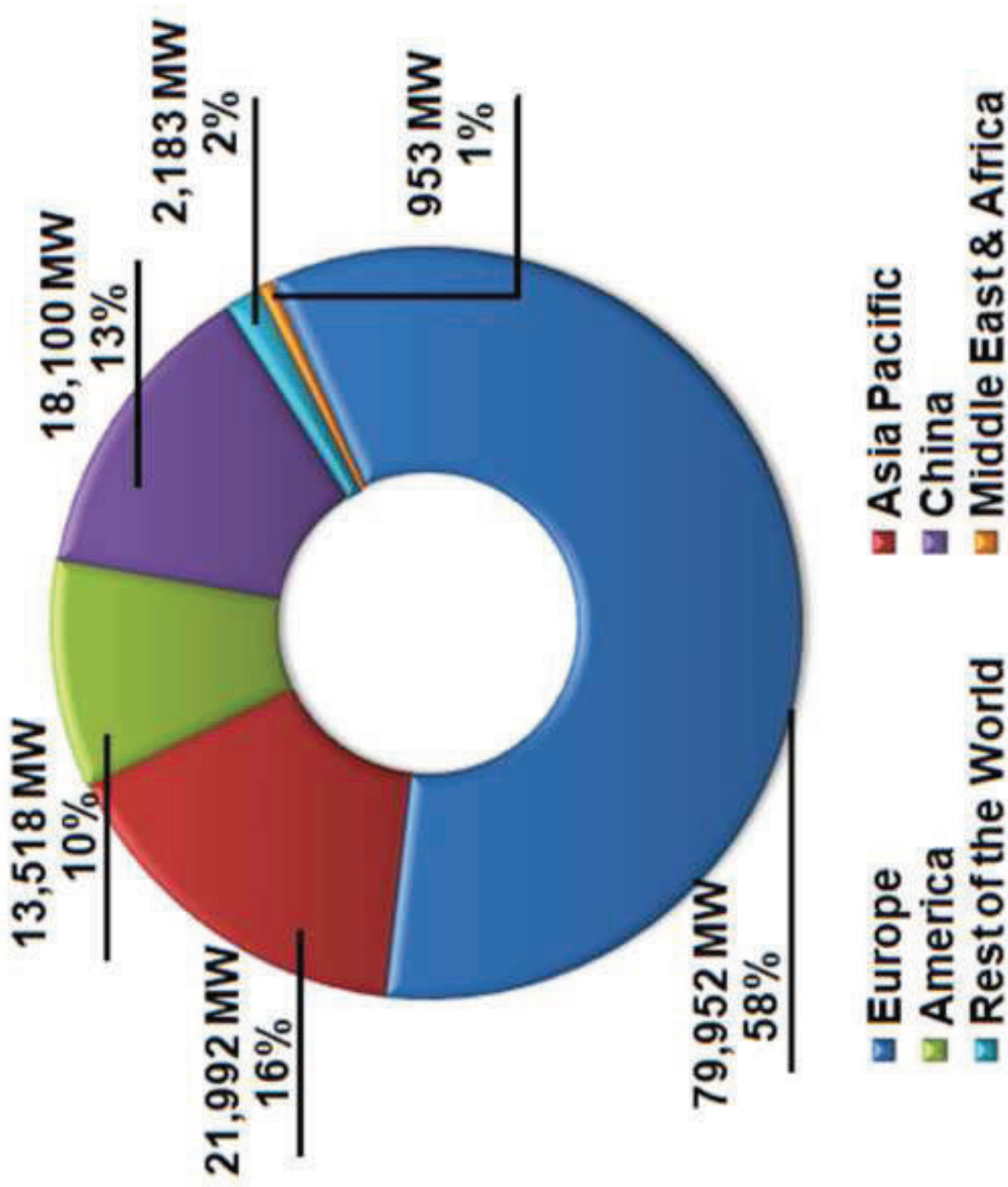


Figure 2  
Click here to download high resolution image

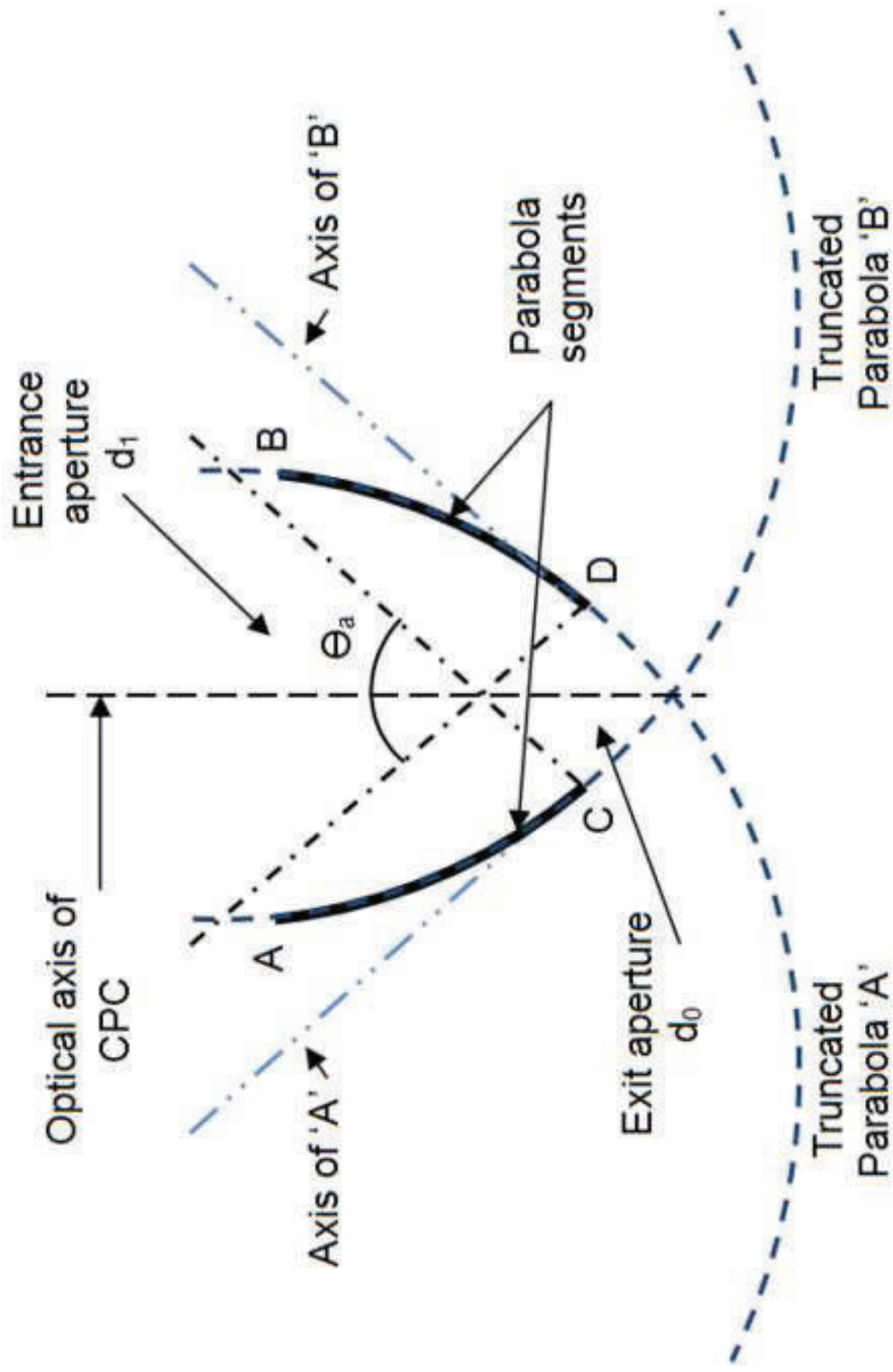


Figure 3  
[Click here to download high resolution image](#)

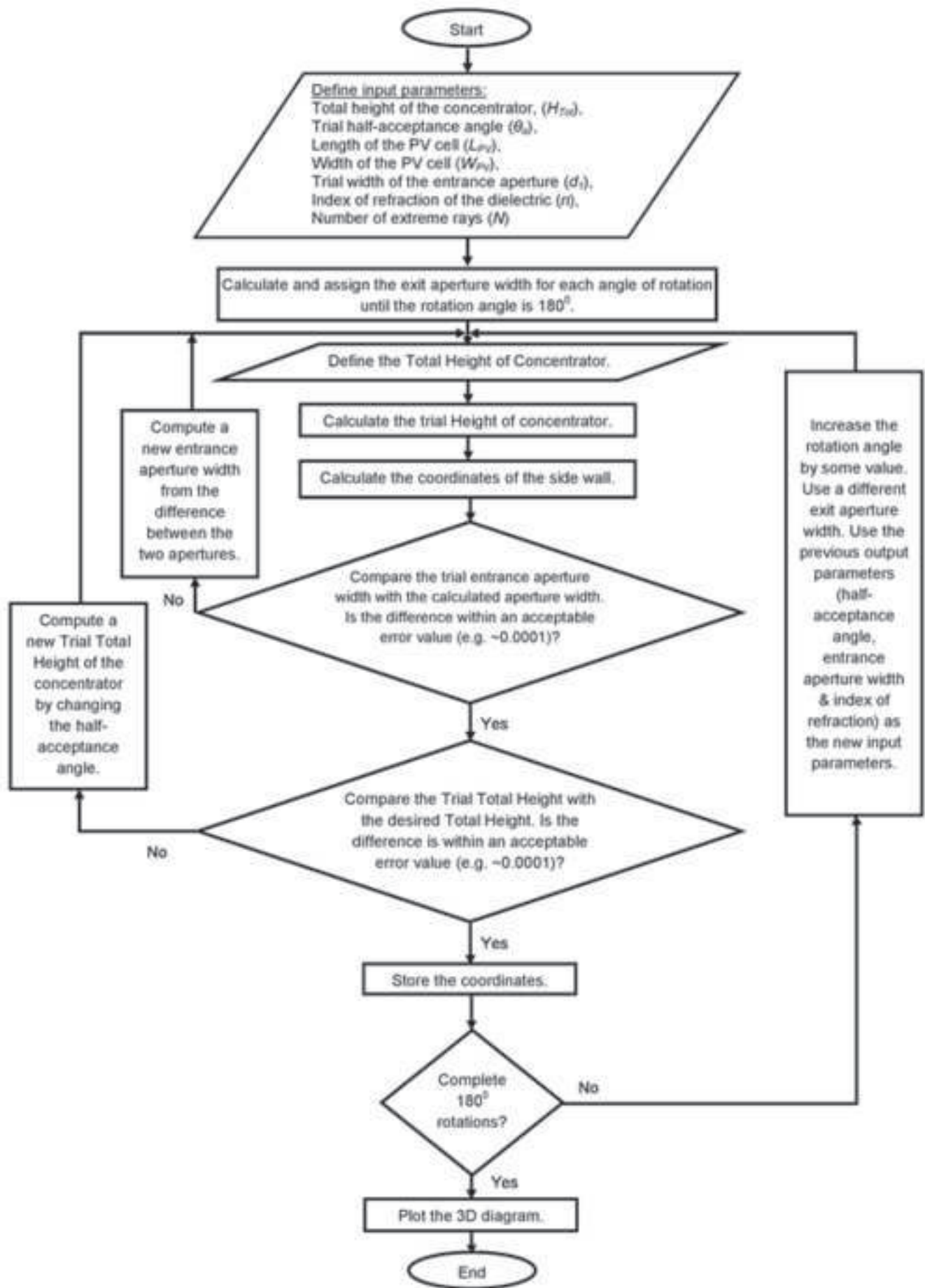


Figure 4  
[Click here to download high resolution image](#)

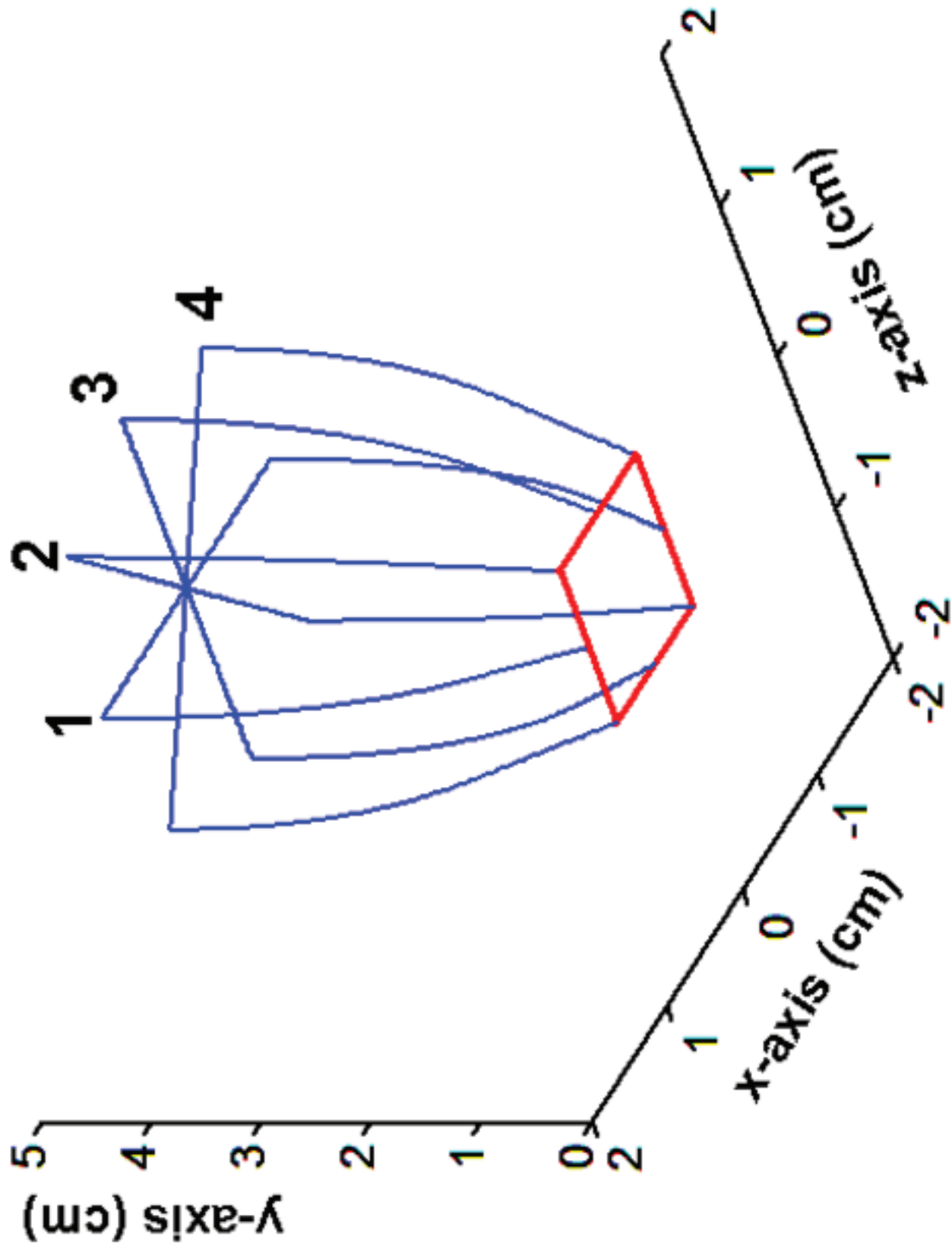


Figure 5  
[Click here to download high resolution image](#)

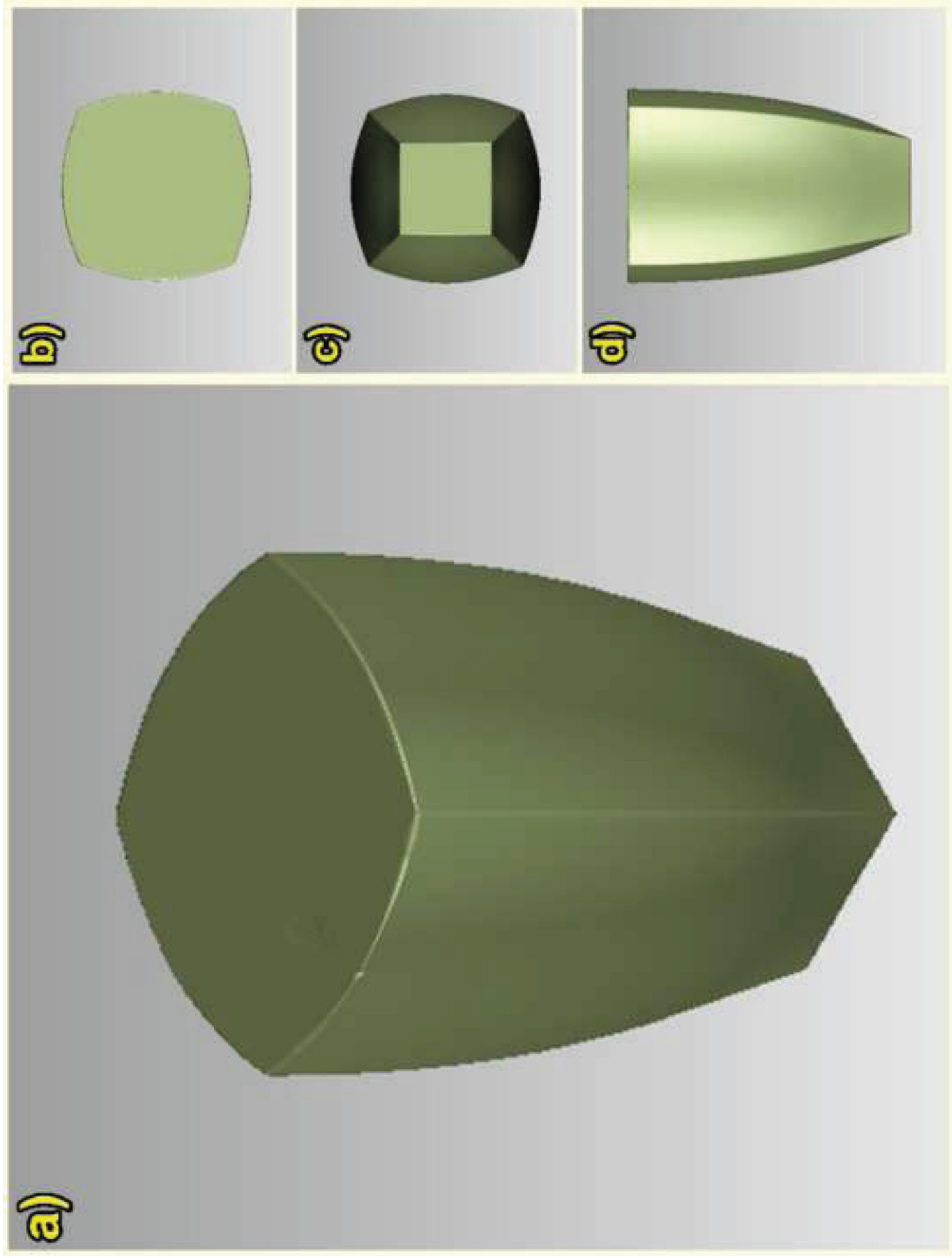
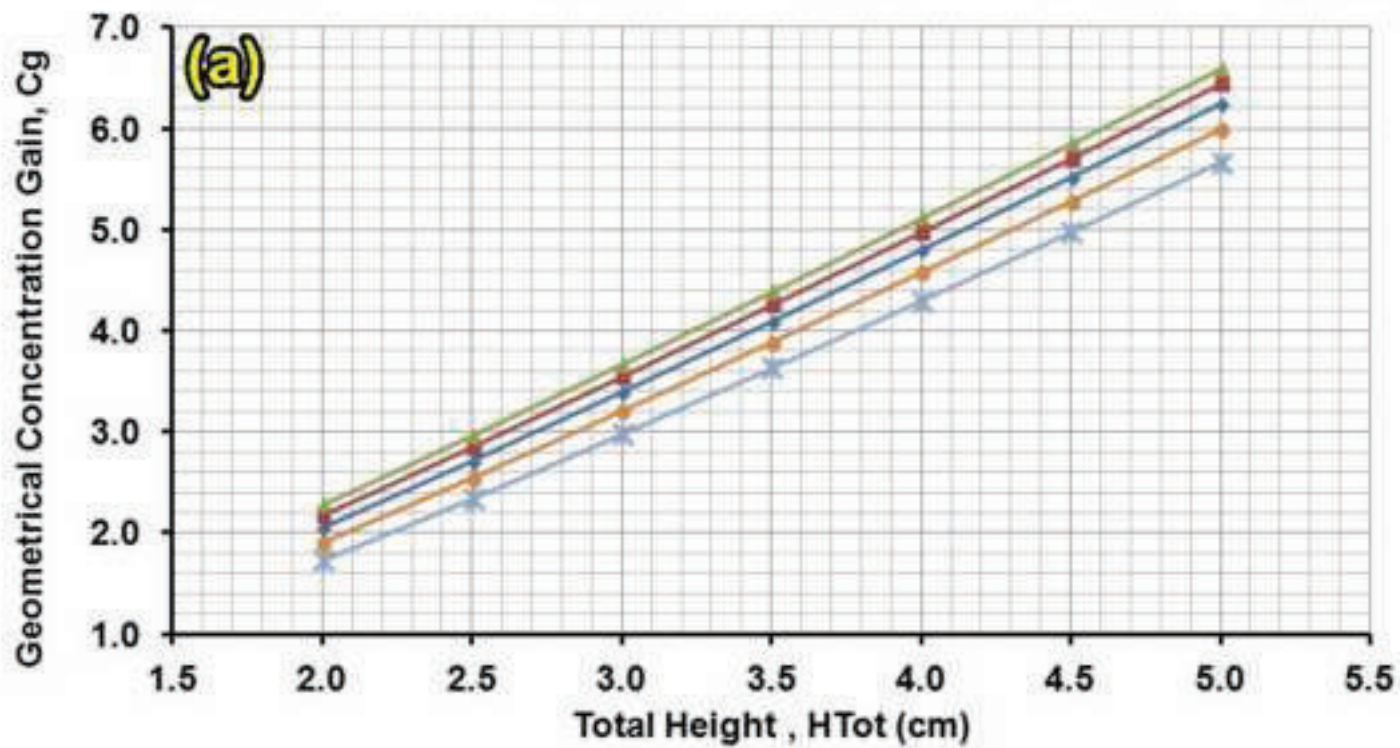
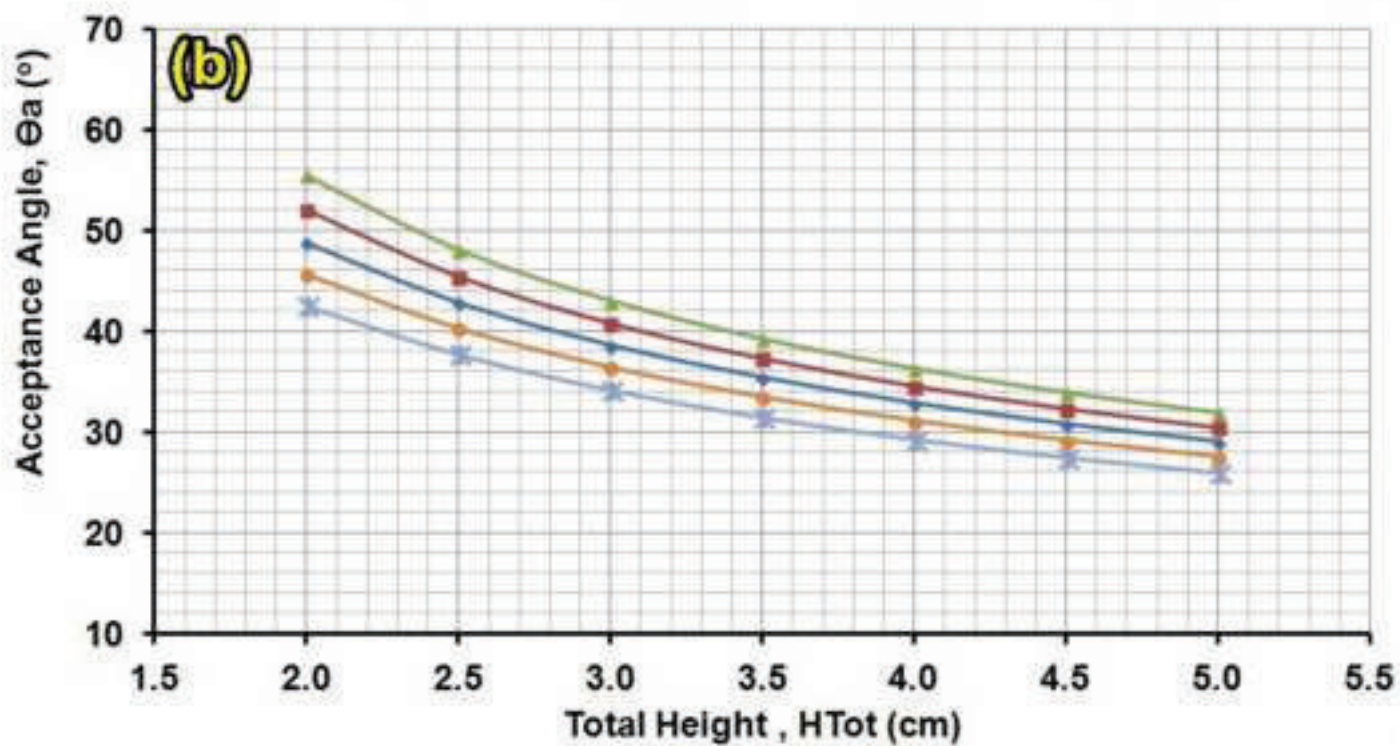




Figure 6  
[Click here to download high resolution image](#)



$n=1.30$     $n=1.35$     $n=1.40$     $n=1.45$     $n=1.50$



$n=1.30$     $n=1.35$     $n=1.40$     $n=1.45$     $n=1.50$

Figure 7  
Click here to download high resolution image

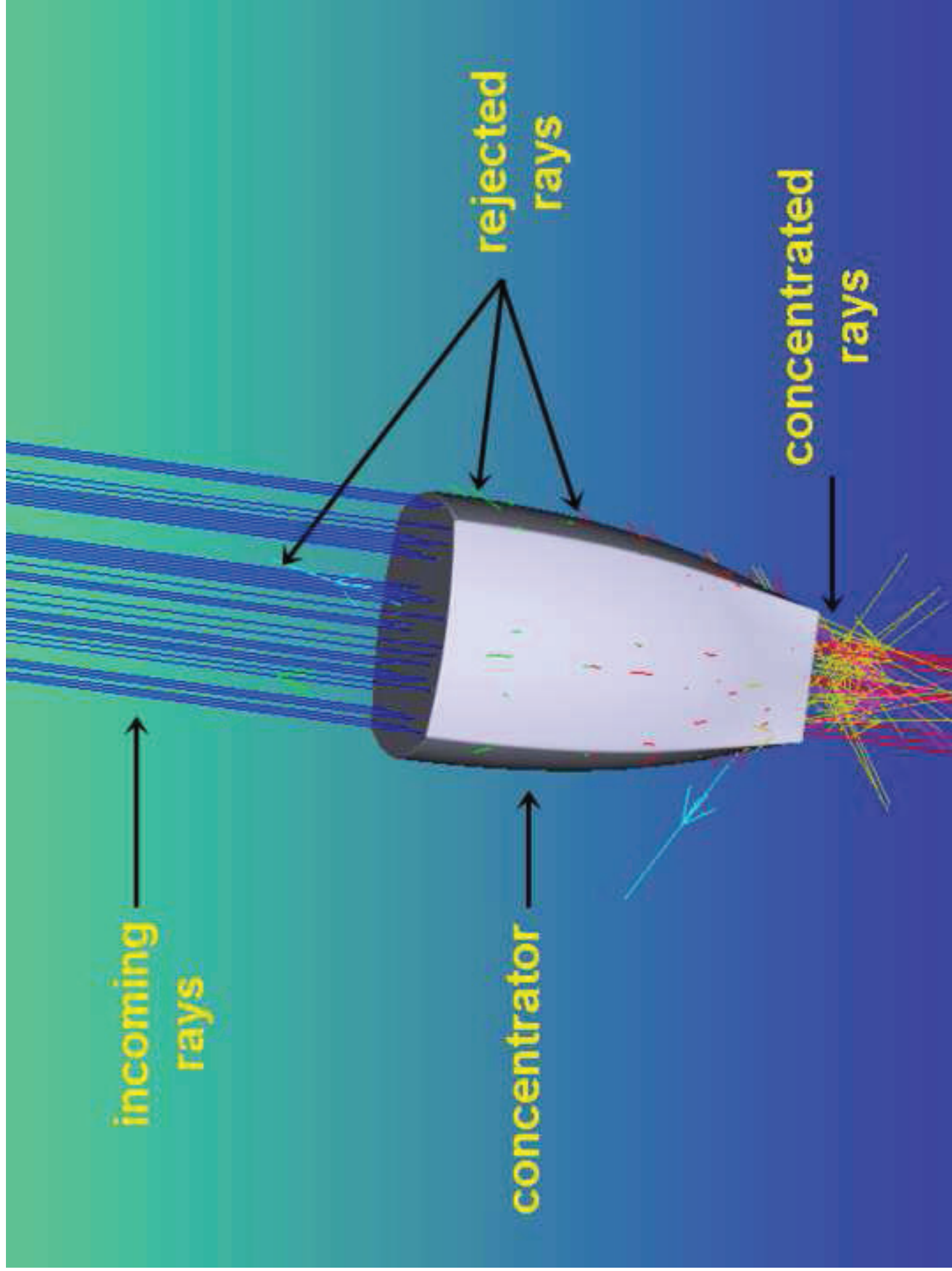




Figure 8

[Click here to download high resolution image](#)

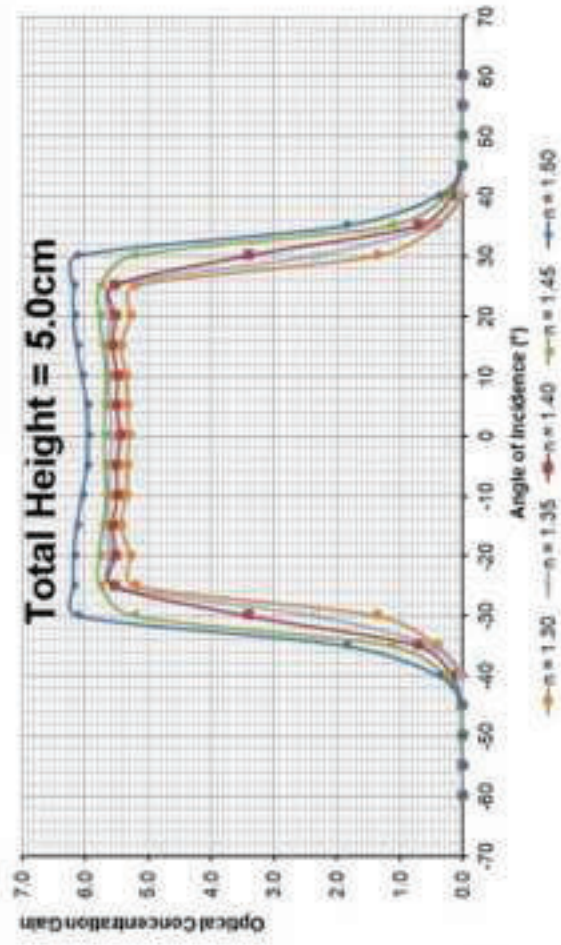
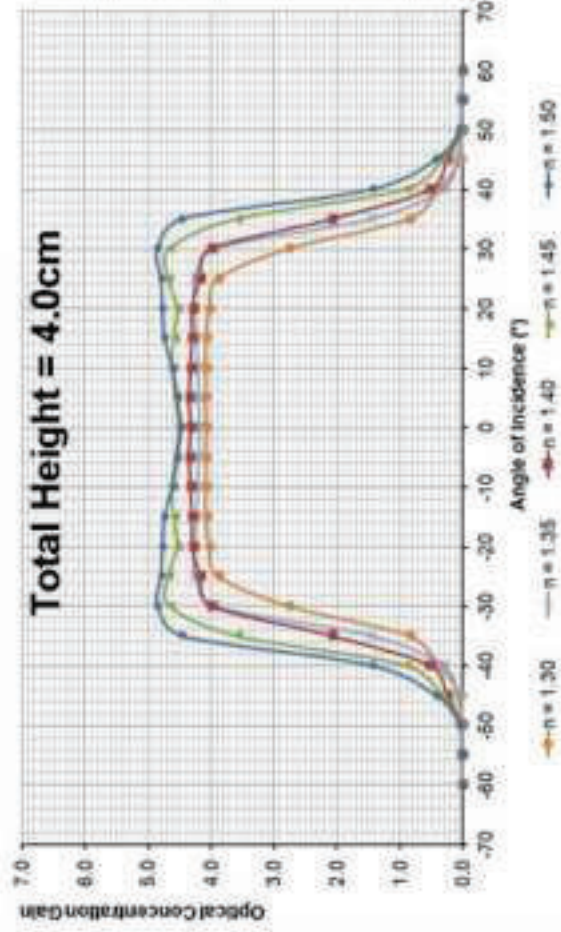
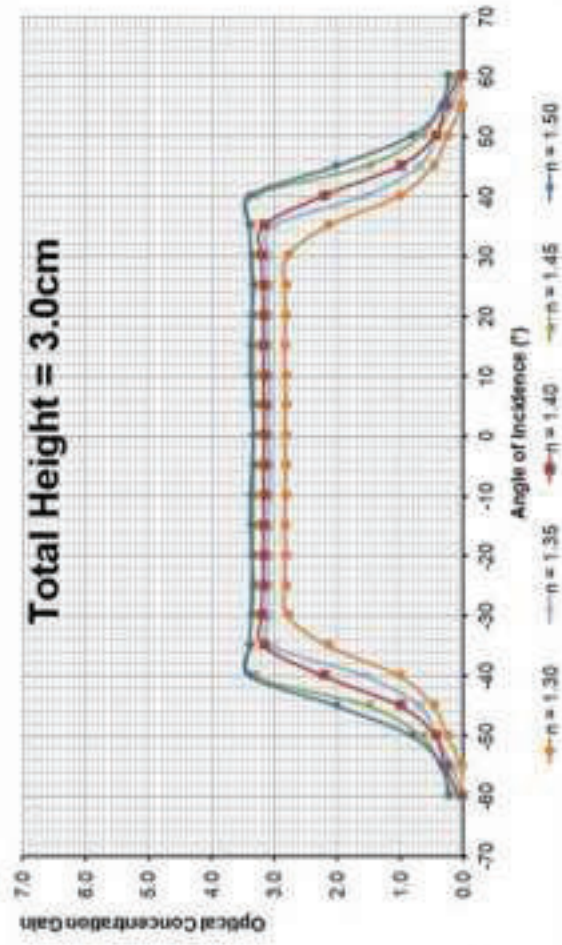
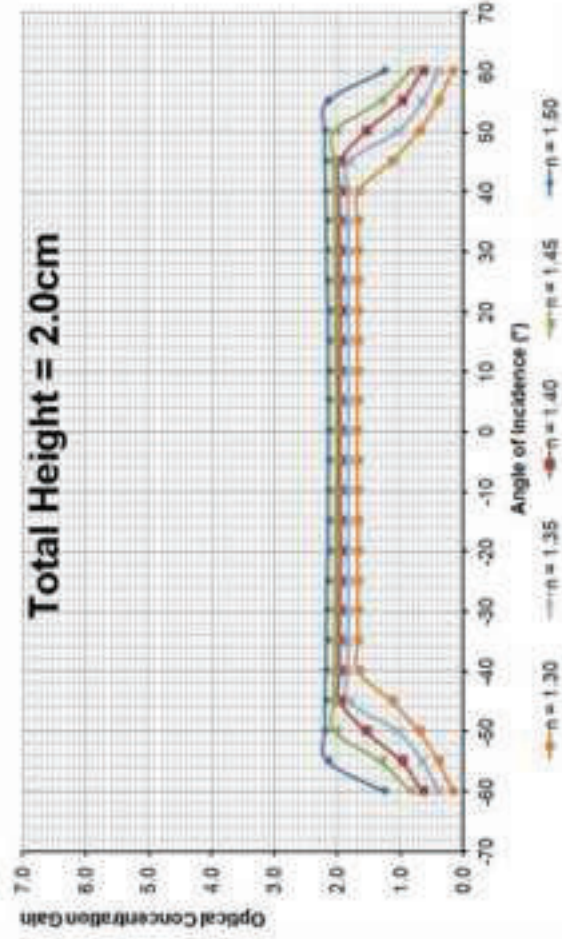




Figure 9  
[Click here to download high resolution image](#)

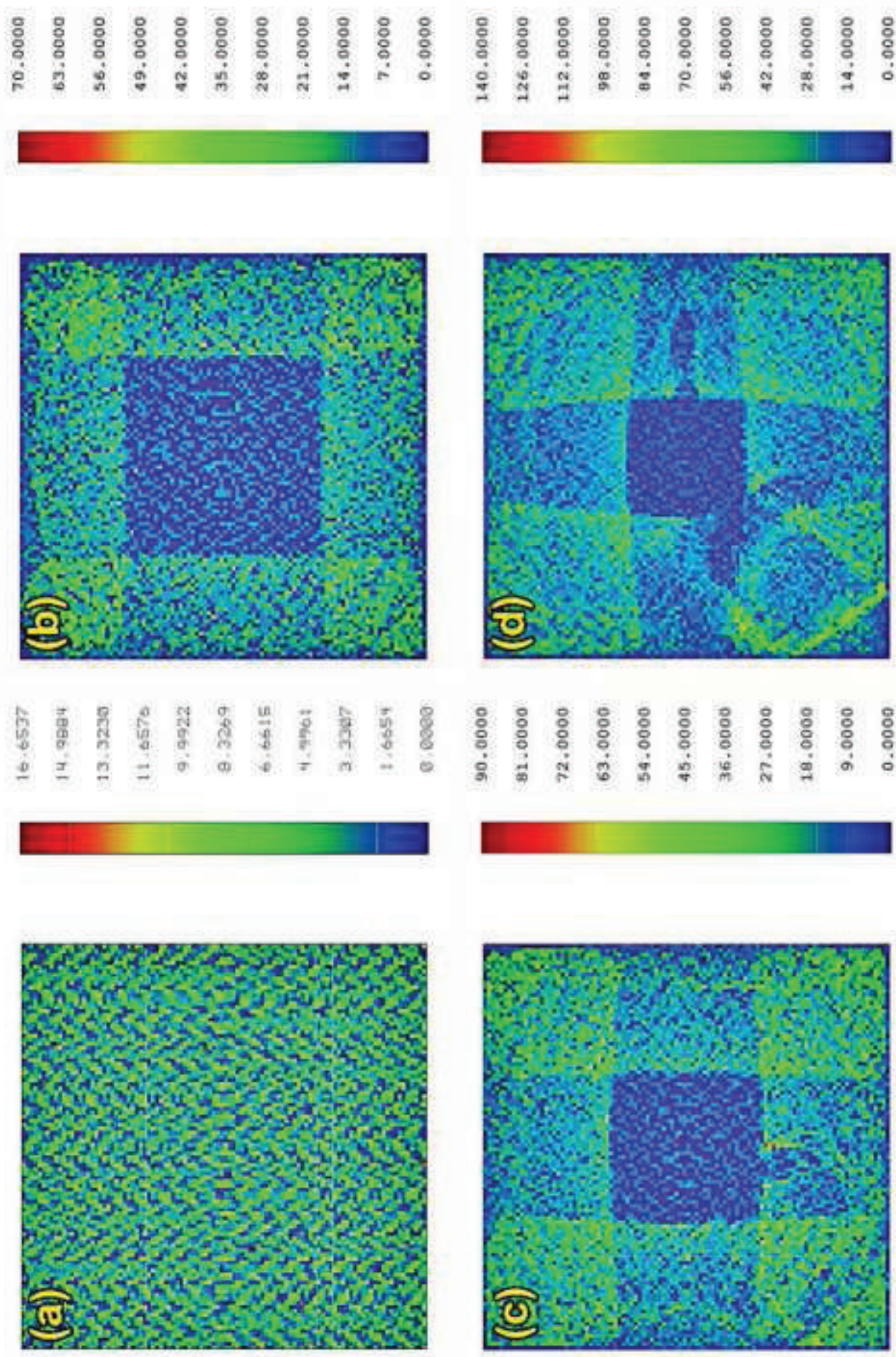


Figure 10  
[Click here to download high resolution image](#)

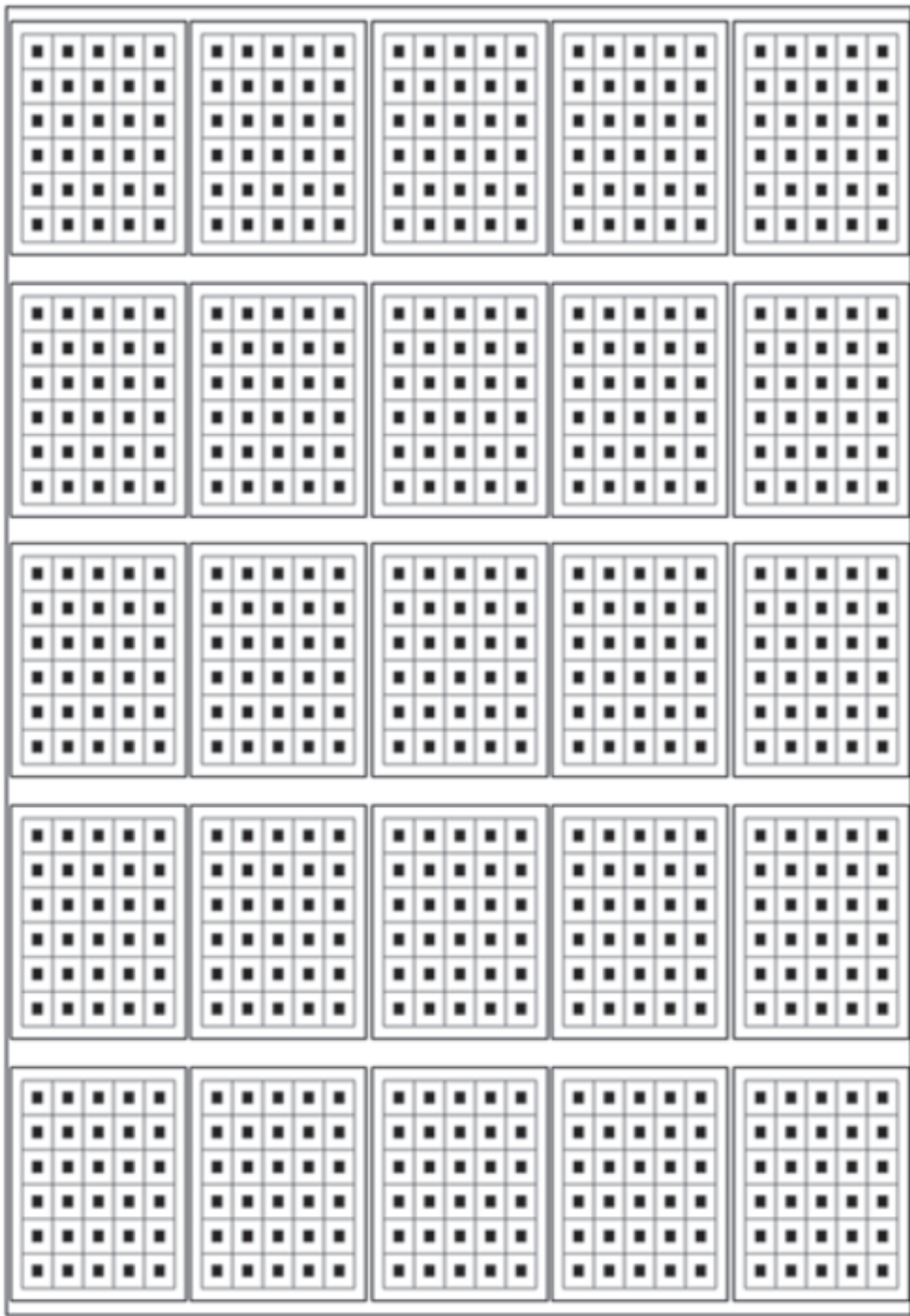




Figure 11  
[Click here to download high resolution image](#)

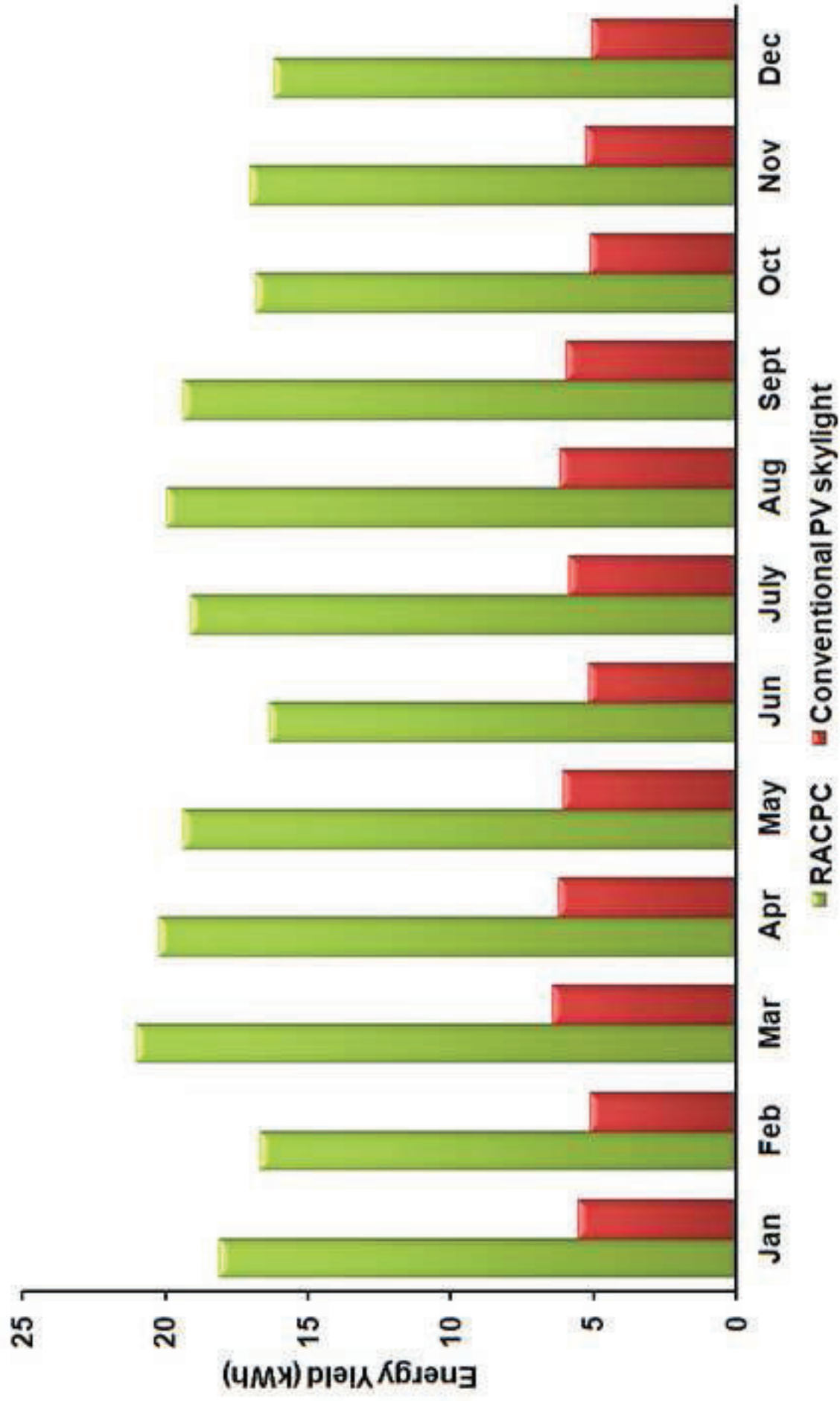


Table 1: Summary of various CPC designs that have been studied.

Authors	Type of CPC	Input parameters	Findings
Ronneld et al. [36]	2D extrusion of a symmetrical reflective CPC.	A geometrical concentration gain of 1.53, an exit aperture width of 14.4 cm, a total height of 12 cm and a half-acceptance angle of 35°.	Increased the annual energy output by 2.6% when compared with the non-concentrating system. This concentrator has a CAP of 0.88.
Pei et al. [37]	2D extrusion of a symmetrical dielectric CPC	A geometrical concentration gain of 2.41, an exit aperture width of 1 cm, total height of 2.7 cm and a half-acceptance angle of 36.8°.	Increased the electrical power from 25.86 mW to 44.80 mW when compared with non-concentrating PV. It is calculated that the CAP of the concentrator is 1.44.
Cooper et al. [38]	Reflective 3D rotationally symmetric CPC	Half-acceptance angle of 30°.	The transmission-angle curve of the reflective design produced an almost ideal step-like behavior within its designed acceptance angle
Goodman et al. [39]	Dielectric 3D rotationally symmetric CPC	A geometrical concentration gain of 6.1, an index of refraction of 1.5 and half-acceptance angle of 10°.	The cell coupled with this CPC design produced a 5.7 more short circuit current when compared with a bare solar cell. This concentrator has a CAP of 0.43.
Mallick et al. [40]	Reflective ACPC.	A geometrical concentration gain of 2.	Increased the maximum electrical output power by 62% when compared with a non-concentrating system, achieving a maximum optical efficiency of 85.85%
Sarmah et al. [41]	Dielectric ACPC	A geometrical concentration gain of 2.8.	Achieved a maximum optical efficiency of 80.5% and increased the electrical power ratio to 2.27 when compared with a system without a concentrator.
Mammo et al. [42]	Reflective 3D CCPC.	A geometrical concentration gain of 3.61, a half-acceptance angle of 30°, a total height of 1.616 cm and a square 1 cm by 1 cm exit aperture.	Generated a maximum power concentration of 3 when compared to similar type of non-concentrating module. The CAP of the concentrator is 0.95.
Baig et al. [43]	Dielectric 3D CCPC.	A geometrical concentration gain of 3.61, a total height of 1.616 cm and a square 1 cm by 1 cm exit aperture.	Achieved a maximum optical efficiency of 73.4%, a half-acceptance angle of 35° and produced a maximum power ratio of 2.67 when compared with the non-concentrating design. The CAP of the concentrator is 1.09.

Table 2

Table 2: Comparison of acceptance angle values generated from the ZEMAX® simulation and from MATLAB® simulation.

Total Height, $HTot$ (cm)	Geometrical concentration gain, $C_g$	Concentration-Acceptance Product, $CAP$	Index of refraction, $n$	Maximum optical efficiency, $C_{opt-eff}$	Half-acceptance angle obtained from ZEMAX®, $\Theta_a$ (°)	Half-acceptance angle obtained from MATLAB®, $\Theta_a$ (°)	Percentage of change (%)
2.00	1.73	0.88	1.30	0.98	42.00	42.50	1.17
	1.90	0.99	1.35	0.96	46.00	45.63	-0.81
	2.05	1.06	1.40	0.96	48.00	48.79	1.62
	2.17	1.16	1.45	0.95	52.00	52.02	0.05
	2.28	1.25	1.50	0.96	56.00	55.39	-1.10
3.00	2.98	0.94	1.30	0.95	33.00	34.13	3.32
	3.21	1.05	1.35	0.97	36.00	36.40	1.10
	3.39	1.11	1.40	0.94	37.00	38.61	4.17
	3.54	1.24	1.45	0.95	41.00	40.79	-0.52
	3.67	1.28	1.50	0.93	42.00	42.96	2.23
4.00	4.30	0.94	1.30	0.95	27.00	29.23	7.62
	4.58	1.07	1.35	0.93	30.00	31.06	3.42
	4.80	1.13	1.40	0.90	31.00	32.83	5.57
	4.97	1.21	1.45	0.93	33.00	34.55	4.47
	5.11	1.30	1.50	0.95	35.00	36.23	3.39
5.00	5.67	1.04	1.30	0.96	26.00	25.92	-0.32
	5.99	1.07	1.35	0.94	26.00	27.49	5.41
	6.25	1.13	1.40	0.89	27.00	28.99	6.85
	6.44	1.27	1.45	0.90	30.00	30.43	1.42
	6.59	1.32	1.50	0.94	31.00	31.84	2.63